

# LONGVILA: SCALING LONG-CONTEXT VISUAL LANGUAGE MODELS FOR LONG VIDEOS

**Anonymous authors**

Paper under double-blind review

## ABSTRACT

Long-context capability is critical for multi-modal foundation models, especially for long video understanding. We introduce LongVILA, a full-stack solution for long-context visual-language models by co-designing the algorithm and system. For model training, we upgrade existing VLMs to support long video understanding by incorporating two additional stages, *i.e.*, long context extension and long video supervised fine-tuning. However, training on long video is computationally and memory intensive. We introduce the long-context Multi-Modal Sequence Parallelism (MM-SP) system that efficiently parallelizes long video training and inference, enabling 2M context length training on 256 GPUs without any gradient checkpointing. LongVILA efficiently extends the number of video frames of VILA from 8 to 2048, achieving 99.8% accuracy in 6,000-frame (more than 1 million tokens) video needle-in-a-haystack. LongVILA-7B demonstrates strong accuracy on 9 popular video benchmarks, *e.g.*, 65.1% VideoMME with subtitle. Besides, MM-SP is  $2.1\times$  -  $5.7\times$  faster than ring style sequence parallelism and  $1.1\times$  -  $1.4\times$  faster than Megatron with a hybrid context and tensor parallelism. Moreover, it seamlessly integrates with Hugging Face Transformers.

## 1 INTRODUCTION

Integrating multi-modal understanding with long-context capability is important. A foundation model supporting more modalities can take more flexible input signals so that people can interact with the model in more diverse manners, *e.g.*, GPT-4o-like multi-modal chatbot, multi-modal web agent (Koh et al., 2024), and real-world robotics foundation model (Brohan et al., 2022; 2023; Padalkar et al., 2023). Longer context enables models to process more information, *e.g.*, long documents, repo-level codebase, and hour-length video, which similarly provides required features to more real-world applications.

While some works have enabled long-context Vision-Language Models (VLMs) (Lin et al., 2023b; Weng et al., 2024), they employ simplified approaches rather than offering a comprehensive solution. For instance, LongVA (Zhang et al., 2024b) relies on long-context LLMs and trains models on short-context data. LongVLM (Weng et al., 2024) utilizes token compression to circumvent context extension. These approaches sidestep more challenging issues, such as the development of a robust long-context multi-modal training framework and corresponding dataset design.

A full-stack design is crucial for long-context Vision-Language Models (VLMs). Training large models is typically a complex, systematic endeavor that demands both data engineering (Betker et al., 2023; Ouyang et al., 2022; Zhou et al., 2024) and system-software co-design (Lepikhin et al., 2020; Chowdhery et al., 2023; Shoeybi et al., 2019; Brown et al., 2020; Dehghani et al., 2023). Unlike text-only LLMs, VLMs (*e.g.*, LLaVA (Liu et al., 2023c)) often require distinct model architectures and flexible distributed training strategies. Additionally, long-context modeling necessitates not only long-context data to fully utilize the model’s capabilities (Fu et al., 2024c; Chen et al., 2023) but also infrastructure capable of supporting memory-intensive long-context training (Li et al., 2021; Jacobs et al., 2023; Li et al., 2023a). Therefore, a full-stack design, encompassing training pipeline and system, is indispensable for long-context VLMs.

In this work, we introduce LongVILA, a comprehensive solution for long-context VLMs. For training **pipeline**, we implement a five-stage training curriculum as Figure 1: (1) multi-modal alignment, (2) large-scale pre-training, (3) short supervised fine-tuning, (4) context extension for LLMs,

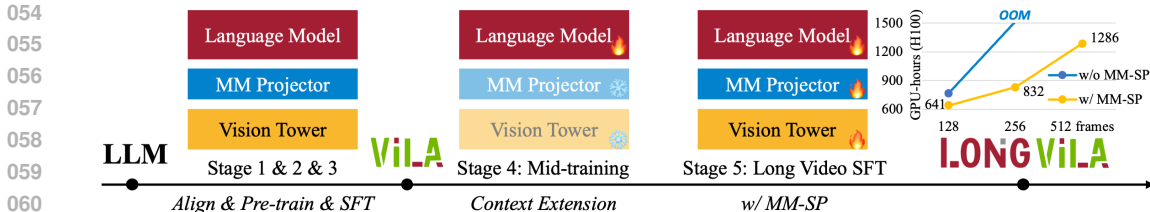


Figure 1: The LongVILA training pipeline. In Stages 1 through 3, the process starts with alignment, pre-training, and supervised fine-tuning. In Stage 4, the model undergoes mid-training context extension. Finally, in Stage 5, the model is fine-tuned for long video understanding with Multi-Modal Sequence Parallelism (MM-SP).

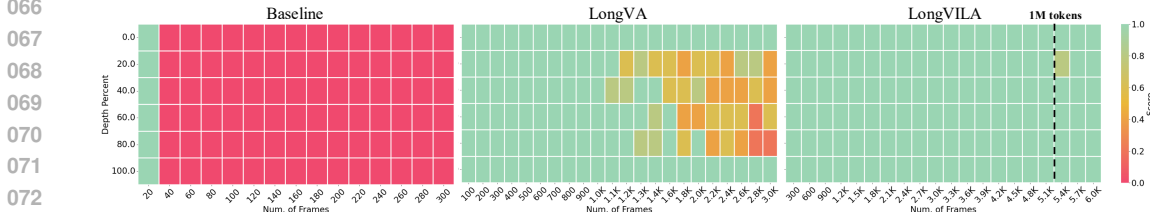


Figure 2: Comparison of Needle in the Long Video Haystack Experiment. The 32-frame baseline model (left) can not retrieve right needles after 32 frames. LongVA (middle) achieves 87.6% accuracy in 3,000 frames. In contrast, the LongVILA model (right), trained on 2048 frames, presents 99.8% accuracy on 6,000 frames (more than 1 million context length).

and (5) long supervised fine-tuning. For **system**, we establish an efficient and user-friendly framework, namely Multi-Modal Sequence Parallelism (MM-SP), which supports training and inferencing memory-intensive long-context VLMs.

LongVILA-7B presents strong performance on 9 popular benchmarks, *e.g.*, 65.1% on VideoMME (Fu et al., 2024a) with subtitle. The LongVILA model, trained on 2048 frames, achieves 99.8% accuracy in the needle-in-a-haystack experiments with 6,000 frames, with a context length of more than 1 million tokens. In ablations, by increasing the number of video frames using LongVILA, the performance on VideoMME in long videos consistently improves (Figure 3). Our MM-SP system can efficiently scale the context length up to 2 million tokens without gradient checkpointing, achieving  $2.1\times$  to  $5.7\times$  speedup compared to ring style sequence parallelism, and  $1.1\times$  to  $1.4\times$  compared to Megatron with a hybrid context parallelism and tensor parallelism.

## 2 RELATED WORKS

**Visual language model architecture.** There are two predominant designs for VLMs: the encoder-decoder architecture (*e.g.*, LLaVA (Liu et al., 2023c), PaLM-E (Driess et al., 2023)) and the decoder-only architecture (*e.g.*, Fuyu (Bavishi et al., 2023), Chameleon (Team, 2024)). Encoder-Decoder VLMs connect the vision encoder to the LLM decoder through a multi-modal projector. Certain multi-modal projectors, such as spatial pooling and Q-former, significantly reduce the number of tokens per image or video frame, thereby lowering the computational burden on the LLM decoder. In contrast, decoder-only LLMs typically process raw patches as input without hierarchical token pooling, making it more challenging to reduce the token count for each image or frame. In this work, we build on VILA (Lin et al., 2023b) as our foundation. It is worth noting that enhanced variants of VILA exist, such as VILA<sup>2</sup>(Fang et al., 2024) for improved performance and X-VILA(Ye et al., 2024) for cross-modality understanding, reasoning, and generation. For our model architecture and training pipeline, we adhere to the standard VILA-1.5 version.

**Sequence parallelism and hybrid strategy.** Long-context training examples often exceed the memory capacity of a single device. To address this issue, the sequence parallelism paradigm has been widely adopted in the text-only LLM community, distributing a single sequence across multiple

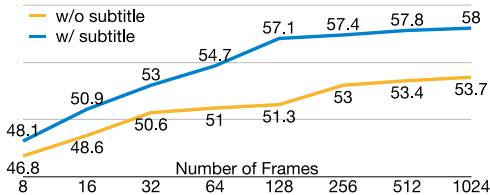


Figure 3: Scaling video frames improves VideoMME accuracy in long category.

Training Stages	VideoMME			
	Average	Short	Medium	Long
1-2-3-4-5	57.5	69.3	56.1	47.0
1-2-4-(3&5)	55.9	67.4	54.1	46.1
4-1-2-3-5	56.0	69.2	54.1	44.5
4-1-2-(3&5)	55.3	67.2	53.6	45.1

Table 1: Ablations on various training stage settings on VideoMME (without subtitle). (3&5) means joint training of the stage 3 and 5.

devices. Specifically, Ring-style systems Li et al. (2021; 2023a); Liu et al. (2023a) use Point-to-Point (P2P) communication primitives to collectively compute the attention module, while DeepSpeed-Ulysses Jacobs et al. (2023) employs an All-to-All (A2A) primitive to alternate between sharding the sequence dimension and the attention head dimension during attention computation. Ulysses generally achieves higher throughput than Ring-style SP due to its more efficient A2A communication primitive and larger, unsegmented computation blocks. However, its scalability is limited by the number of attention heads. Recently, USP (Fang & Zhao, 2024) was introduced as the first to integrate Ring-style SP and Ulysses SP, combining the strengths of both approaches. LoongTrain (Gu et al., 2024) further optimizes communication and placement strategies to enhance training efficiency. Following (Fang & Zhao, 2024; Gu et al., 2024), we extend the system to multi-modal scenarios to accommodate complex attention masks and variable-length input sequences. Our work is the first to design and implement a sequence parallelism system for visual language models.

### 3 LONGVILA TRAINING PIPELINE

As shown in Figure 1, in our pipeline, there are five training stages, *i.e.*, Stage 1: multi-modal alignment, Stage 2: large-scale pre-training, Stage 3: supervised fine-tuning, Stage 4: context extension for LLM, Stage 5: long supervised fine-tuning. Stage 1, 2, and 3 follow VILA (Lin et al., 2023b), to firstly bridge the gap between LLM and vision encoder, and then pre-training on larger datasets. In Stage 1, only the multi-modal projector is trainable with others frozen. In Stage 2, we freeze the vision encoder and training LLM and the multi-modal projector. In Stage 3, we fully fine-tune the model for short data instruction following, *e.g.*, image and short video datasets. Afterwards, we extend the context length of LLM with text-only dataset in a continued pre-training manner in Stage 4. In Stage 5, we adopt our MM-SP system (§4) to enhance the instruction following abilities by long video supervised fine-tuning. It is noted that all parameters are trainable in the final stage.

#### 3.1 STAGE1&2&3: ALIGNMENT, PRE-TRAINING, AND SHORT SUPERVISED FINE-TUNING

We first use open-sourced image and video caption datasets to train the multi-modal projector in stage (1) to conduct the multi-modal alignment. Note that, following (Lin et al., 2023b), both vision encoder and LLM decoder are frozen at this stage. After that, we conduct large-scale pre-training to learn general multi-modal capacity at scale. To improve the quality of large open-sourced datasets, we follow VILA<sup>2</sup> (Fang et al., 2024) to relabel COYO-25M (Lin et al., 2023b; Byeon et al., 2022) with VILA-1.5-40B (Lin et al., 2023b). The supervised fine-tuning process incorporates mixed data types, including both images and videos. For short video comprehension, we utilize open-source video instruction-following datasets, *e.g.*, YouCook2 Zhou et al. (2018) and ShareGPTVideo Zhang et al. (2024c). In experiments, our model is based on Qwen2-1.5B and Qwen2-7B (qwe, 2024).

#### 3.2 STAGE4: CONTEXT EXTENSION FOR LLMs

Our empirical research indicates that extending the context length of LLMs is essential prior to engaging in supervised fine-tuning with long video datasets. Following Stage 2 of our methodology, we execute a continuation of pre-training on the LLM to enhance its context length to 262,144, utilizing a total of 17B tokens. We employ a progressive training schedule, incrementally increasing the context length from 8,192 to 65,536, and ultimately to 262,144, utilizing the SlimPajama dataset (Soboleva et al., 2023) in accordance with the methodology outlined by (Fu et al., 2024d).



Figure 4: The proportion of question and video categories in our LongVILA\_sft dataset. We have 15,292 videos in total. For each video, there are one sample for captioning and the other question.

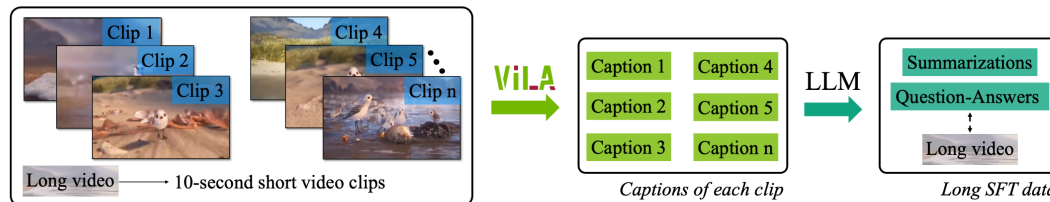


Figure 5: The pipeline for generating instruction-following data from long videos. The process begins by segmenting the long video into short clips, each approximately 10 seconds in length. These clips are individually annotated with captions using the VILA-1.5 model. Subsequently, a Large Language Model (LLM) is employed to generate question-and-answer pairs based on the captions of these clips. The types of questions generated include summarization and other inquiries pertinent to the content of long videos.

Furthermore, we augment the base frequency of the Rotary Position Embeddings (RoPE) as described in (Su et al., 2021) during the fine-tuning phase. Sequence parallelism is implemented for the training at the 262,144 context length. We use low-rank adaptation for context extension fine-tuning (Chen et al., 2024b). These processes collectively require approximately 336 GPU hours on machines equipped with 80GB A100 GPUs.

### 3.3 STAGE5: LONG SUPERVISED FINE-TUNING

**Long video instruction following** To facilitate the fine-tuning of long videos, we constructed a new, dedicated dataset for long video training, each consisting of 15,292 videos. We use the original long videos from the Shot2Story dataset (Han et al., 2023). Each video includes different questions and answers: one for generating captions and another for answering questions, enabling diverse applications in video understanding. Figure 5 illustrates the process for generating instruction-following datasets from long videos. Initially, the long video is segmented into shorter clips, each approximately 10 seconds in duration. These clips are then independently annotated with descriptive captions utilizing the VILA-1.5 model. Subsequently, an LLM is employed to generate question-and-answer pairs derived from the captions of these clips. The generated questions encompass summarization and other queries relevant to the comprehensive understanding of long video content.

As in Figure 4, the left chart categorizes videos into several domains, including Travel & Events, Sports, Education, Pets & Animals, People & Blogs, News & Politics, Music, Science & Technology, Comedy, Entertainment, Film, and Gaming, ensuring a wide-ranging representation of video content. The right chart breaks down the categories of questions into Spatial, Attribute, Action, Object, OCR, Synopsis, and Temporal, reflecting the variety of inquiries and cognitive tasks that the dataset can address. This dataset provides a rich resource for advancing the understanding and processing of long video formats in supervised fine-tuning.

Once we acquired the long video dataset, applying it for supervised fine-tuning introduced new challenges, primarily due to the substantial number of frames in each sample—often ranging in the hundreds or even thousands. For instance, a single sequence from 1400 video frames can encompass around 274k tokens. Existing data-parallel training systems struggle to handle such extensive contexts. We developed the MM-SP system (Section 4) to efficiently train long-context VLMs.

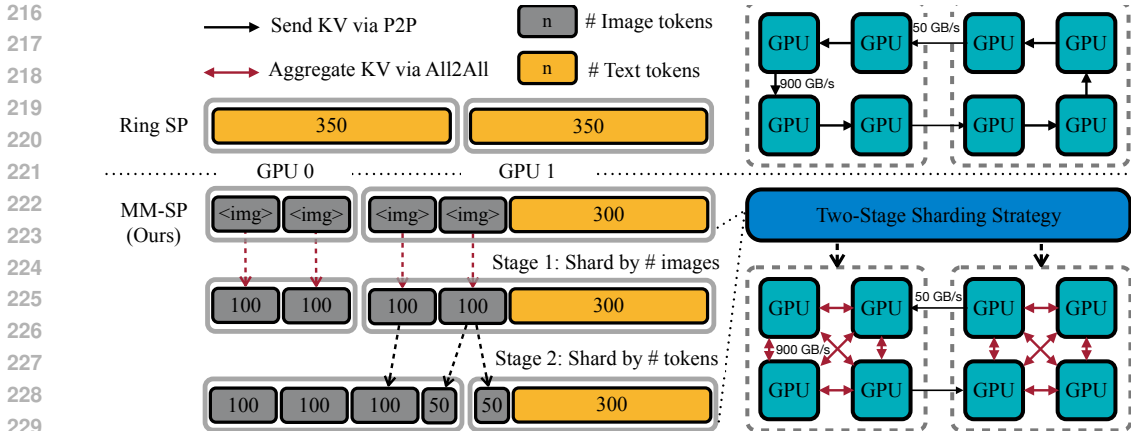


Figure 6: Sharding strategy and communication pattern of MM-SP. For sharding strategy, Ring SP is designed for text-only modalities, without optimization for the workload of an image encoder. Our MM-SP implements a novel sharding strategy that balances the computational load between the image encoder and the language modeling stages. For communication pattern, Ring SP (Liu et al., 2023a; Li et al., 2023a) (top) relies on P2P communication for both intra-node and inter-node settings, resulting in underutilization of intra-node bandwidth. MM-SP (bottom) adopts 2D-Attention (Fang & Zhao, 2024; Gu et al., 2024) mechanism which utilizes intra-node All-to-All (All2All) and inter-node Point-to-Point (P2P) communication to transfer keys and values (KV), enhancing the efficiency of intra-node NVLink utilization. The bandwidth is for H100.

## 4 MULTI-MODAL SEQUENCE PARALLELISM

Training long-context Vision-Language Models (VLMs) results in substantial memory demands. The most widely used open-source solution, fully sharded data parallelism, does not distribute the activations generated by a single sequence, making it unsuitable for our needs. Consequently, we developed a custom system based on sequence parallelism (Li et al., 2021; 2023a; Liu et al., 2023a; Jacobs et al., 2023), a technique commonly employed in existing foundation model systems to optimize text-only LLM training. However, we discovered that existing systems are neither efficient nor scalable enough to handle our long-context VLM workloads.

### 4.1 LIMITATIONS OF EXISTING SYSTEMS

In this section, we address the inefficiencies of current sequence-parallel systems when applied to multi-modal LLMs.

**Modality heterogeneity.** In text-only LLMs, sequences are processed by a single tokenizer into tokens, allowing for straightforward distribution of tokens across multiple GPUs. However, VLMs incorporate an encoder architecture where non-text data is initially represented by a placeholder token (e.g., `<img>`) and subsequently encoded into multiple real tokens during training. For instance, a single video frame typically requires around 256 tokens (Lin et al., 2023b). Due to the differing processing requirements of visual and text modalities, a simplistic implementation that treats placeholder tokens the same as text tokens leads to an imbalance in GPU workloads (Figure 6).

**Networking heterogeneity.** Our multi-modality comprises extremely long videos (Figure 1), which requires employing sequence parallelism in a *multi-node* setting. In a multi-node setting, inter-node and intra-node network bandwidth differs significantly. For example, the NVIDIA DGX H100 utilizes NVLink at 900 GB/s for intra-node GPU communication and InfiniBand at 50 GB/s for inter-node GPU communication (single path), resulting in an  $18\times$  difference in bandwidth. Previous work, Ring-Style sequence parallelism (Li et al., 2021; 2023a; Liu et al., 2023a; Zhu, 2023) ignores the heterogeneous networking feature on GPUs and utilizes P2P communication in both inter-node and intra-node settings. This design induces excessive communication costs where they usually attempt to overlap them into computation. However, we found that this design cannot always hide the overhead, and even slows down the computation kernel (Table 2).



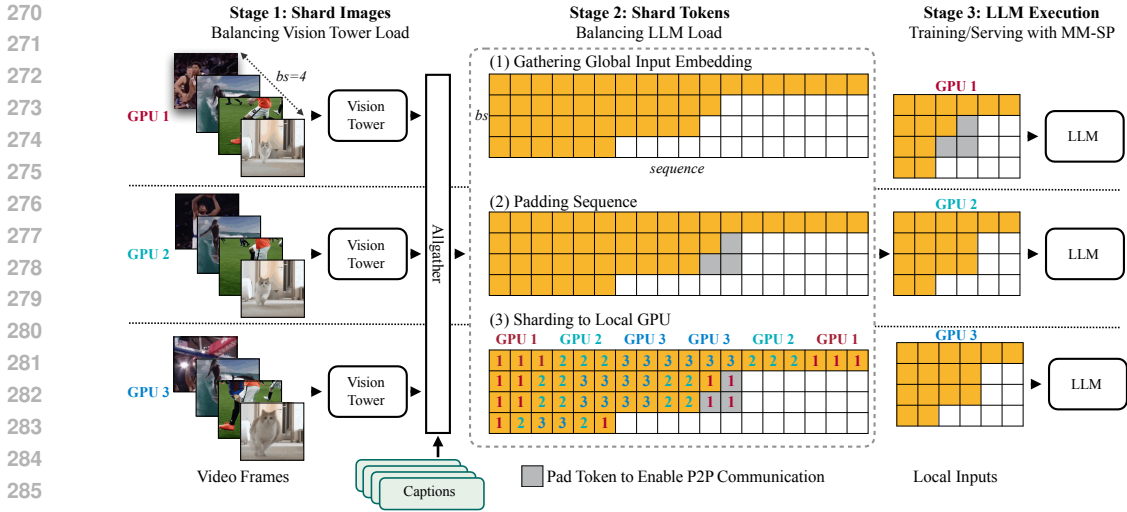


Figure 7: Workflow of Multi-Modal Sequence Parallelism with a Batch Size (bs) of 4 and a Sequence Parallel Size (SP\_Size) of 3. To accommodate multi-modal inputs, we developed a customized sharding strategy that ensures balanced workload distribution and compatibility with SP communication.

**Limited maximal sequence length.** DeepSpeed-Ulysses (Jacobs et al., 2023) presents a potential solution to the communication challenges in ring-style sequence parallelism by employing All-to-All communication primitives, which reduce the overall communication volume. However, this approach has its limitations. The design relies on parallelizing along the attention head dimension rather than the sequence dimension during attention computation. As a result, DeepSpeed-Ulysses cannot scale effectively beyond the number of attention heads. For instance, the Llama-3 8B model uses Grouped Query Attention (GQA) with 8 Key-Value heads, which restricts the maximum sequence parallelism degree to 8. Even when using replication for Key-Value heads, which introduces additional communication overhead (Li et al., 2023a), the highest achievable sequence parallelism degree is still limited to 32 (the number of Query heads). This constraint is insufficient for handling extremely long sequences, such as full-length movies.

#### 4.2 MULTI-MODAL SEQUENCE PARALLELISM TRAINING MODE

After identifying the limitations in existing systems, we conclude that an ideal multi-modal sequence parallelism approach should prioritize efficiency and scalability by addressing both modality and network heterogeneity, and should also be capable of scaling beyond the number of attention heads. To achieve this, we adopt 2D-attention (Fang & Zhao, 2024; Gu et al., 2024) mechanism for sequence parallelism. For instance, as illustrated on the left in Figure 6, to enable an 8-degree sequence parallelism across 2 nodes, we construct a  $4 \times 2$  communication mesh using 2D-SP. In this setup, the A2A process group, with a size of 4, distributes the QKV tensors according to the head dimension and re-partitions them along the sequence dimension within each node. Simultaneously, the P2P process group, with a size of 2, transfers the partitioned KV chunks between nodes. Additionally, to further explain how the 2D-attention mechanism operates, we depict the attention computation schedule using different methods in Figure 11.

**MM-SP workflow.** To address the challenge of modality heterogeneity, we propose a two-stage sharding strategy that optimizes the compute workload for both image encoding and language modeling stages. As illustrated in Figure 7, the process begins by evenly distributing images (e.g., video frames) across devices within the sequence parallelism (SP) process group, thereby achieving load balancing during the image encoding stage. In the second stage, we aggregate global vision and text inputs for token-level sharding. To support ring-based attention, sequences are extended with arbitrary dummy tokens, ensuring that each sequence can be evenly divided according to the ring-based SP degree. This adjustment maintains consistency with the original approach by modifying label inputs to ignore padded tokens during loss calculation. We implement a balanced sharding strategy that distributes the context to each rank from both ends, ensuring equal computation across ranks.

Table 2: The forward and backward attention kernel wall-clock time with or without the overlapping design (Unit:  $\mu s$ ). The communication overlap design in Ring-style SP **slows down** the attention kernel by occupying streaming multiprocessor (SM) resources.

Seq. length	4K	8K	16 K	24K	32K
forw. w/o	29.5	49.3	122.1	239.2	402.9
forw. w/	35.0 (+18.6%)	54.6 (+10.7%)	131.2 (+7.5%)	250.9 (+4.8%)	420.1 (+4.2%)
backw. w/o	77.7	123.3	362.9	730.0	1218.9
backw. w/	82.2 (+5.8%)	129.8 (+5.3%)	367.0 (+1.1%)	743.2 (+1.8%)	1225.3 (+0.5%)

The effectiveness of this strategy will be demonstrated later (Table 5). Since this redistribution is performed only once during training, the overhead is minimal. Finally, the balanced local inputs are processed by the LLM backbone, utilizing 2D-Attention to achieve efficient sequence parallelism.

### 4.3 MULTI-MODAL SEQUENCE PARALLELISM INFERENCE MODE

The model we developed through sequence parallelism training is capable of handling long-context multi-modal downstream tasks. However, the most commonly used inference system, built on HuggingFace Transformers, typically operates on a single GPU. This lack of distributed implementation limits the maximum sequence length that can be processed during inference. The most straightforward solution within HuggingFace Transformers is to use its pipeline parallelism inference feature, which shards a single model across multiple devices on a layer-by-layer basis (Huang et al., 2019; Narayanan et al., 2019). However, this approach is inefficient, as it only activates one GPU at a time. Additionally, it struggles to support long sequence because the first device must store large input embeddings and images, creating a memory bottleneck.

To address these limitations, we implemented sequence parallelism for distributed inference in VLMs. Unlike the training mode, the inference system additionally manages tensors, such as input tokens and position encodings, that progressively change during the decoding phase (Yu et al., 2022). It detects signals from the machine with the last token to terminate the distributed process appropriately. Compared to HuggingFace’s pipeline parallelism strategy, our inference mode is more efficient, as all devices participate in computation simultaneously, accelerating the process by a factor proportional to the number of machines (Figure 8). Furthermore, it is scalable, with memory evenly distributed across devices, enabling longer sequences with additional machines.

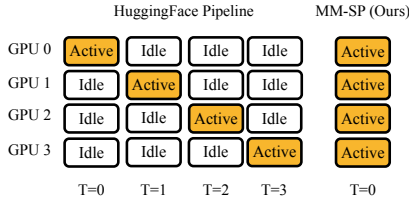


Figure 8: Inference scheduling comparison between HuggingFace Pipeline and MM-SP, illustrated with 4 GPUs. MM-SP utilizes all GPUs concurrently.

## 5 EXPERIMENTAL RESULTS

We evaluate our full-stack solution from both system and modeling perspectives. First, we present our training and inference results to demonstrate the efficiency and scalability of our system, which enables long-context training and inference. We then assess the performance of our long-context model on captioning and instruction-following tasks.

### 5.1 TRAINING AND INFERENCE SYSTEM

Our training and inference systems can be integrated with HuggingFace Transformers through straightforward monkey patching, in line with the popular open-source approach outlined in (Zheng et al., 2023). In this section, we present a quantitative evaluation of the training system’s throughput, the inference system’s latency, and the maximum supported sequence length.

378  
379  
380  
381  
382  
383  
384  
385  
386  
387  
388  
389  
390  
391  
392  
393  
394  
395  
396  
397  
398  
399  
400  
401  
402  
403  
404  
405  
406  
407  
408  
409  
410  
411  
412  
413  
414  
415  
416  
417  
418  
419  
420  
421  
422  
423  
424  
425  
426  
427  
428  
429  
430  
431

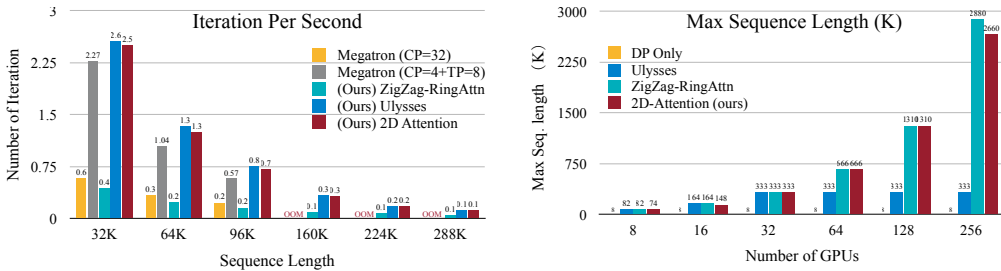


Figure 9: Performance comparison of training systems on 32 H100 GPUs. MM-SP is as scalable as ZigZag-RingAttn, and as efficient as Ulysses.

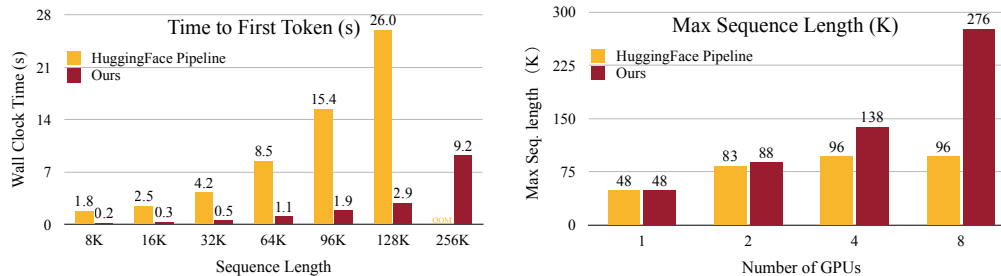


Figure 10: Performance comparison of inference systems on 8 H100 GPUs.

### 5.1.1 TRAINING SYSTEM

**Baselines and hardware setup** For training efficiency, we compare our system with ZigZag ring-style sequence parallelism, which incorporates load balancing and GPU optimization (ZIGZAG-RINGATTN for consistency)(Li et al., 2023a; Zhu, 2023; Liu et al., 2024a; Korthikanti et al., 2023). We use a widely adopted open-source implementation (Zhu, 2023). To reduce the memory footprint of models, gradients, and optimizer states, we employ Fully-Sharded Data Parallelism (FSDP)(Zhao et al., 2023) instead of Zero-3(Rajbhandari et al., 2020) (Table 7). Additionally, we compare our system with the expert-designed and highly optimized Megatron-LM(Shoeybi et al., 2019; Korthikanti et al., 2023) system, focusing on their implementation of sequence parallelism, termed “context parallelism” (CP). We also evaluate a hybrid strategy that combines tensor model parallelism (TP) within a node and CP across nodes, as recommended by the Megatron-LM team for advanced usage.

We conduct most experiments on H100 nodes, each equipped with 8xH100 (80GB) GPUs interconnected via intra-node NVLink and 400 Gbps inter-node InfiniBand. For experiments involving the maximum supported sequence length during training, we extend the setup to 32 A100 nodes, each with 8xA100 (80GB) GPUs, where the conclusions are consistent with those for H100 due to the equivalent total memory. Our evaluations are based on an 8B model with a batch size of 1. Since the Megatron-LM baseline does not natively support VLM training and the visual encoder is typically orders of magnitude smaller than LLMs, we report the main results for the LLM backbone without the visual encoder. An ablation study of the visual encoder is provided in § 5.1.3.

**Throughput** Figure 9 presents throughput results measured as iteration per second over 32 H100 GPUs. These results were obtained after 10 warmup iterations and averaged over 5 iterations to minimize variance. Our system achieves a speedup of  $2.1\times$  to  $5.7\times$  compared to ZIGZAG-RINGATTN, and performs on par with DeepSpeed-Ulysses. When compared to the more optimized ring-style sequence parallelism in Megatron-LM CP, our method shows a  $3.1\times$  to  $4.3\times$  speedup. This highlights that our system design effectively addresses the issues inherent in ring-style sequence parallelism, as in § 4.2. Furthermore, our system achieves a  $1.1\times$  to  $1.4\times$  speedup compared to Megatron-LM’s hybrid strategy. Note that our system is currently implemented in Triton (Tillet et al., 2019), and further porting it to C++ could yield even greater speedup. Additionally, we observed that the Megatron-LM system supports a significantly lower maximum sequence length, which is why its results are not in the next section. We observe similar observations using 8 H100 nodes (Table 8).



Table 3: Performance comparisons on 9 video benchmarks, including ActivityNet-QA (Yu et al., 2019), EgoSchema (Mangalam et al., 2023), EventBench (Du et al., 2024), LongVideoBench (Wu et al., 2024), PerceptionTest (Patraucean et al., 2023), MVBench (Li et al., 2024b), NExT-QA (Xiao et al., 2021), VNBench (Zhao et al., 2024), and VideoMME (Fu et al., 2024a).

Model	LLM Size	ActNet-QA	EgoSchema	EventBench	LVideoBench	PercepTest	MVBench	NExT-QA	VNBench	VideoMME	
		test	test	val	val	val	test	mc	val	w/o sub.	w/ sub.
GPT-4V	-	57.0	-	32.6	61.3	-	43.5	-	-	59.9	63.3
GPT-4o	-	-	-	53.3	66.7	-	-	-	64.4	71.9	77.2
Gemini-1.5-Pro	-	57.5	72.2	43.2	64.0	-	-	-	66.7	75.0	81.3
Video-LLaVA	7B	45.3	38.4	5.9	37.6	-	43.5	-	12.4	39.9	41.6
Flash-VStream	7B	51.9	-	-	-	-	-	61.6	-	-	-
ShareGPT4Video	8B	50.8	-	-	41.8	-	51.2	-	-	39.9	43.6
VideoLLaMA2	7B	50.2	51.7	6.9	-	51.4	54.6	-	4.5	47.9	50.3
VideoLLaMA2.1	7B	53.0	53.1	-	-	54.9	57.3	-	-	54.9	56.4
Kangaroo	8B	-	62.7	-	54.8	-	61.1	-	-	56.0	57.6
PLLaVA	7B	56.3	-	28.2	39.2	-	46.6	-	-	-	-
LLaVA-OV	7B	56.7	60.1	-	56.4	57.1	56.7	79.4	51.8	58.2	61.5
LongVILA	7B	<b>59.5</b>	<b>67.7</b>	<b>58.0</b>	<b>57.1</b>	<b>58.1</b>	<b>67.1</b>	<b>80.7</b>	<b>63.0</b>	<b>60.1</b>	<b>65.1</b>

We evaluate the maximum sequence length supported by a fixed number of GPUs by progressively increasing the per-GPU sequence length from 1k to 10k until an out-of-memory error occurs. The results are summarized in Figure 9. To ensure a fair comparison, activation checkpointing is disabled. Vanilla data parallelism fails to scale for long videos at larger cluster sizes. DeepSpeed-Ulysses partitions based on attention heads, which limits its ability to scale to higher context lengths, as the 8B model has only 32 attention heads. Consequently, our approach supports approximately  $8\times$  higher context lengths when scaled to 256 GPUs. Additionally, our system achieves a similar context length scaling as ZIGZAG-RINGATTN, with support for over **2 million** context length on 256 GPUs.

In summary, our training system combines the best of both worlds—it achieves scalability comparable to ZIGZAG-RINGATTN while maintaining the throughput of DeepSpeed-Ulysses. Additionally, it delivers a  $1.3\times$  speedup and supports  $2.5\times$  longer context lengths compared to the highly optimized Megatron-LM.

### 5.1.2 INFERENCE SYSTEM

We evaluated our inference system against HuggingFace Pipeline parallelism using a single node with 8 H100 GPUs and the 8B model (Figure 10). Our system achieves an  $8.2\times$  speedup compared to HuggingFace Pipeline on 8xH100 GPUs. This significant improvement is primarily due to HuggingFace Pipeline inference activating only one GPU at a time, whereas our method leverages all GPUs to compute jointly. Figure 10 compares the maximum supported sequence length, where our method supports sequences that are  $2.9\times$  longer than those supported by HuggingFace Pipeline. Specifically, during 96K sequence length inference, HuggingFace Pipeline stores 80GB of activations on the first GPU and only 18GB on the remaining GPUs. This imbalanced allocation of activations limits the maximum supported sequence length.

### 5.1.3 EFFECT OF TWO-STAGE SHARDING

We evaluate the impact of our two-stage sharding strategy using a video captioning dataset (Chen et al., 2024a). We compare our two-stage sharding to a one-stage baseline that only distributes workload based on the number of images. We measure the time per iteration across different numbers of H100 GPUs. For  $k$  GPUs, we use  $k$  images per video and a batch size of  $k$ . The results, shown in Table 5, indicate a speedup ranging from 1% to 7%. This improvement is primarily observed

Table 4: Performance comparison on VideoMME (Fu et al., 2024a) benchmark in details.

Model	LLM Size	Frames	<i>w/o subtitle</i>				<i>w subtitle</i>			
			Overall	Short	Medium	Long	Overall	Short	Medium	Long
Video-LLaVA	7B	8	39.9	45.3	38.0	36.2	41.6	46.1	40.7	38.1
SliME	8B	8	45.3	53.3	<u>55.4</u>	39.8	47.2	55.4	44.4	41.7
ShareGPT4Video	8B	16	39.9	48.3	36.3	35.0	43.6	53.6	39.3	37.9
VideoChat2	7B	16	39.5	48.3	37.0	33.2	43.8	52.8	39.4	39.2
VideoLLaMA2	7B	16	47.9	56.0	45.4	42.1	50.3	59.4	47.6	43.8
Chat-Univi-v1.5	7B	64	40.6	45.7	40.3	35.8	45.9	51.2	44.6	41.8
Kangaroo	8B	64	<u>56.0</u>	66.1	55.3	46.7	<u>57.6</u>	68.0	55.4	49.3
ShareGemini	7B	64	43.2	49.1	41.3	39.1	47.9	49.1	47.3	43.4
LongVA	7B	128	52.6	61.1	50.4	46.2	54.3	61.1	53.6	47.6
InternVL-V1.5	20B	10	50.7	60.2	46.4	45.6	52.4	61.7	49.1	46.6
VITA	8x7B	20	55.0	64.2	53.3	<u>47.6</u>	57.6	67.9	55.3	<u>49.6</u>
Video-CCAM	14B	96	53.9	62.1	52.8	47.0	56.1	63.9	<u>55.9</u>	48.3
LongVILA	1.5B 7B	256	<u>53.6</u> <b>60.1</b>	<u>66.2</u> <b>69.0</b>	<u>49.3</u> <b>58.3</b>	<u>45.3</u> <b>53.0</b>	<u>57.5</u> <b>65.1</b>	<u>70.2</u> <b>72.9</b>	<u>54.1</u> <b>64.9</b>	<u>48.2</u> <b>57.4</b>

in longer captioning tasks, where the baseline suffers from workload imbalance due to the lack of sharding based on the number of text tokens.

## 5.2 GENERAL VIDEO UNDERSTANDING

Table 3 presents the performance of LongVILA, comparing to state-of-the-art models (Lin et al., 2023a; Zhang et al., 2024d; Chen et al., 2024a; Li et al., 2023c; Cheng et al., 2024; Jin et al., 2023; Zhang et al.; Share, 2024; Chen et al., 2024c; Fu et al., 2024b; Fei et al., 2024; Liu et al., 2024c; Xu et al., 2024; Li et al., 2024a; Zhang et al., 2024a) on popular video benchmarks. LongVILA-7B achieves strong performance across all these benchmarks. Table 4 compares their effectiveness across short, medium, and long video lengths, as well as overall performance on VideoMME. LongVILA, utilizing 256 frames, achieves an overall score of 60.1 / 65.1 without / with subtitle, which are competitive results. We include LongVILA-1.5B (starting from Qwen2-1.5B (qwe, 2024)) for evaluation, which is also competitive. We provide a detailed model complexity of LongVILA among various model size, number of frames, context length, latency and FLOPs in Table 10 in the appendix. We also do the ablation on training schedules in Table 1.

## 5.3 NEEDLE-IN-A-HAYSTACK

In Figure 2, we present the results of the Needle in a Haystack experiment for long videos. Following the methodology established in the existing literature (Zhang et al.), we prepared a long video and sampled a fixed number of frames. We inserted specifically designed images at various depths and tasked the model with answering corresponding questions. The 32-frame baseline model (left) was unable to accurately retrieve the correct images beyond 32 frames. In contrast, the LongVILA model (right) demonstrated 99.8% accuracy across 6,000 frames, which contains more than 1 million tokens. To our best knowledge, this is the first VLM which can handle 1 million context length.

## 6 CONCLUSION

We introduce LongVILA, a comprehensive full-stack solution for long-context visual language models, encompassing model training pipeline and distributed system. Based on our curated long video datasets and five-stage training pipeline, our LongVILA model extends the feasible frame count from 8 to 2048, precisely capturing fine-grained information from 2-hour needle-in-a-haystack videos, with more than 1 million tokens. Our LongVILA-7B model achieves strong performance across popular video benchmarks, especially on VideoMME, e.g., 65.1% accuracy with subtitle. Our system efficiently scales context length up to 2 million tokens, achieving speedups of  $2.1\times$  to  $5.7\times$  compared to ring sequence parallelism and  $1.1\times$  to  $1.4\times$  compared to a hybrid Megatron context and tensor parallelism.

## REFERENCES

- 540  
541  
542 Qwen2 technical report. 2024.
- 543  
544 Jinze Bai, Shuai Bai, Shusheng Yang, Shijie Wang, Sinan Tan, Peng Wang, Junyang Lin, Chang  
545 Zhou, and Jingren Zhou. Qwen-vl: A frontier large vision-language model with versatile abilities.  
546 *arXiv preprint arXiv:2308.12966*, 2023.
- 547  
548 Rohan Bavishi, Erich Elsen, Curtis Hawthorne, Maxwell Nye, Augustus Odena, Arushi Somani,  
549 and Sağnak Taşlılar. Introducing our multimodal models, 2023.
- 550  
551 James Betker, Gabriel Goh, Li Jing, Tim Brooks, Jianfeng Wang, Linjie Li, Long Ouyang, Juntang  
552 Zhuang, Joyce Lee, Yufei Guo, et al. Improving image generation with better captions. *Computer  
553 Science*. <https://cdn.openai.com/papers/dall-e-3.pdf>, 2(3):8, 2023.
- 554  
555 Anthony Brohan, Noah Brown, Justice Carbajal, Yevgen Chebotar, Joseph Dabis, Chelsea Finn,  
556 Keerthana Gopalakrishnan, Karol Hausman, Alex Herzog, Jasmine Hsu, et al. Rt-1: Robotics  
557 transformer for real-world control at scale. *arXiv preprint arXiv:2212.06817*, 2022.
- 558  
559 Anthony Brohan, Noah Brown, Justice Carbajal, Yevgen Chebotar, Xi Chen, Krzysztof Choromanski,  
560 Tianli Ding, Danny Driess, Avinava Dubey, Chelsea Finn, et al. Rt-2: Vision-language-action  
561 models transfer web knowledge to robotic control. *arXiv preprint arXiv:2307.15818*, 2023.
- 562  
563 Tom Brown, Benjamin Mann, Nick Ryder, Melanie Subbiah, Jared D Kaplan, Prafulla Dhariwal,  
564 Arvind Neelakantan, Pranav Shyam, Girish Sastry, Amanda Askell, et al. Language models are  
565 few-shot learners. *Advances in neural information processing systems*, 33:1877–1901, 2020.
- 566  
567 Minwoo Byeon, Beomhee Park, Haecheon Kim, Sungjun Lee, Woonhyuk Baek, and Saehoon Kim.  
568 Coyo-700m: Image-text pair dataset, 2022.
- 569  
570 Lin Chen, Xilin Wei, Jinsong Li, Xiaoyi Dong, Pan Zhang, Yuhang Zang, Zehui Chen, Haodong  
571 Duan, Bin Lin, Zhenyu Tang, et al. Sharegpt4video: Improving video understanding and genera-  
572 tion with better captions. *arXiv preprint arXiv:2406.04325*, 2024a.
- 573  
574 Yukang Chen, Shengju Qian, Haotian Tang, Xin Lai, Zhijian Liu, Song Han, and Jiaya Jia. Longlora:  
575 Efficient fine-tuning of long-context large language models. *arXiv preprint arXiv:2309.12307*,  
576 2023.
- 577  
578 Yukang Chen, Shengju Qian, Haotian Tang, Xin Lai, Zhijian Liu, Song Han, and Jiaya Jia. Longlora:  
579 Efficient fine-tuning of long-context large language models. In *The International Conference on  
580 Learning Representations*, 2024b.
- 581  
582 Zhe Chen, Weiyun Wang, Hao Tian, Shenglong Ye, Zhangwei Gao, Erfei Cui, Wenwen Tong,  
583 Kongzhi Hu, Jiapeng Luo, Zheng Ma, Ji Ma, Jiaqi Wang, Xiaoyi Dong, Hang Yan, Hwei Guo,  
584 Conghui He, Botian Shi, Zhenjiang Jin, Chao Xu, Bin Wang, Xingjian Wei, Wei Li, Wenjian  
585 Zhang, Bo Zhang, Pinlong Cai, Licheng Wen, Xiangchao Yan, Min Dou, Lewei Lu, Xizhou Zhu,  
586 Tong Lu, Dahua Lin, Yu Qiao, Jifeng Dai, and Wenhai Wang. How far are we to gpt-4v? closing  
587 the gap to commercial multimodal models with open-source suites. *CoRR*, abs/2404.16821,  
588 2024c.
- 589  
590 Zesen Cheng, Sicong Leng, Hang Zhang, Yifei Xin, Xin Li, Guanzheng Chen, Yongxin Zhu, Wenqi  
591 Zhang, Ziyang Luo, Deli Zhao, and Lidong Bing. Videollama 2: Advancing spatial-temporal  
592 modeling and audio understanding in video-llms. *CoRR*, abs/2406.07476, 2024.
- 593  
Aakanksha Chowdhery, Sharan Narang, Jacob Devlin, Maarten Bosma, Gaurav Mishra, Adam  
Roberts, Paul Barham, Hyung Won Chung, Charles Sutton, Sebastian Gehrmann, et al. Palm:  
Scaling language modeling with pathways. *Journal of Machine Learning Research*, 24(240):  
1–113, 2023.
- Wenliang Dai, Junnan Li, Dongxu Li, Anthony Meng Huat Tiong, Junqi Zhao, Weisheng Wang,  
Boyang Albert Li, Pascale Fung, and Steven C. H. Hoi. Instructblip: Towards general-purpose  
vision-language models with instruction tuning. *ArXiv*, abs/2305.06500, 2023.

- 594 Tri Dao. Flashattention-2: Faster attention with better parallelism and work partitioning. In *ICLR*,  
595 2024.
- 596 Mostafa Dehghani, Josip Djolonga, Basil Mustafa, Piotr Padlewski, Jonathan Heek, Justin Gilmer,  
597 Andreas Peter Steiner, Mathilde Caron, Robert Geirhos, Ibrahim Alabdulmohsin, et al. Scaling  
598 vision transformers to 22 billion parameters. In *International Conference on Machine Learning*,  
599 pp. 7480–7512. PMLR, 2023.
- 600 Danny Driess, Fei Xia, Mehdi SM Sajjadi, Corey Lynch, Aakanksha Chowdhery, Brian Ichter,  
601 Ayzaan Wahid, Jonathan Tompson, Quan Vuong, Tianhe Yu, et al. Palm-e: An embodied multi-  
602 modal language model. *arXiv preprint arXiv:2303.03378*, 2023.
- 603 Yifan Du, Kun Zhou, Yuqi Huo, Yifan Li, Wayne Xin Zhao, Haoyu Lu, Zijia Zhao, Bingning Wang,  
604 Weipeng Chen, and Ji-Rong Wen. Towards event-oriented long video understanding. *CoRR*,  
605 abs/2406.14129, 2024.
- 606 Jiarui Fang and Shangchun Zhao. Usp: A unified sequence parallelism approach for long context  
607 generative ai. *arXiv preprint arXiv:2405.07719*, 2024.
- 608 Yunhao Fang, Ligeng Zhu, Yao Lu, Yan Wang, Pavlo Molchanov, Jang Hyun Cho, Marco Pavone,  
609 Song Han, and Hongxu Yin. Vila<sup>2</sup>: Vila augmented vila. *arXiv preprint arXiv:2407.17453*, 2024.
- 610 Jiajun Fei, Dian Li, Zhidong Deng, Zekun Wang, Gang Liu, and Hui Wang. Video-ccam: Enhancing  
611 video-language understanding with causal cross-attention masks for short and long videos. *CoRR*,  
612 abs/2408.14023, 2024.
- 613 Chaoyou Fu, Yuhan Dai, Yondong Luo, Lei Li, Shuhuai Ren, Renrui Zhang, Zihan Wang, Chenyu  
614 Zhou, Yunhang Shen, Mengdan Zhang, Peixian Chen, Yanwei Li, Shaohui Lin, Sirui Zhao,  
615 Ke Li, Tong Xu, Xiawu Zheng, Enhong Chen, Rongrong Ji, and Xing Sun. Video-mme: The  
616 first-ever comprehensive evaluation benchmark of multi-modal llms in video analysis. *CoRR*,  
617 abs/2405.21075, 2024a.
- 618 Chaoyou Fu, Haojia Lin, Zuwei Long, Yunhang Shen, Meng Zhao, Yifan Zhang, Xiong Wang,  
619 Di Yin, Long Ma, Xiawu Zheng, Ran He, Rongrong Ji, Yunsheng Wu, Caifeng Shan, and Xing  
620 Sun. VITA: towards open-source interactive omni multimodal LLM. *CoRR*, abs/2408.05211,  
621 2024b.
- 622 Yao Fu, Rameswar Panda, Xinyao Niu, Xiang Yue, Hannaneh Hajishirzi, Yoon Kim, and Hao Peng.  
623 Data engineering for scaling language models to 128k context. *arXiv preprint arXiv:2402.10171*,  
624 2024c.
- 625 Yao Fu, Rameswar Panda, Xinyao Niu, Xiang Yue, Hannaneh Hajishirzi, Yoon Kim, and Hao Peng.  
626 Data engineering for scaling language models to 128k context. *CoRR*, abs/2402.10171, 2024d.
- 627 Diandian Gu, Peng Sun, Qinghao Hu, Ting Huang, Xun Chen, Yingtong Xiong, Guoteng Wang,  
628 Qiaoling Chen, Shangchun Zhao, Jiarui Fang, Yonggang Wen, Tianwei Zhang, Xin Jin, and Xu-  
629 anzhe Liu. Loongtrain: Efficient training of long-sequence llms with head-context parallelism.  
630 *CoRR*, pdf/2406.18485, 2024.
- 631 Mingfei Han, Linjie Yang, Xiaojun Chang, and Heng Wang. Shot2story20k: A new benchmark for  
632 comprehensive understanding of multi-shot videos. *arXiv preprint arXiv:2311.17043*, 2023.
- 633 Yanping Huang, Youlong Cheng, Ankur Bapna, Orhan Firat, Dehao Chen, Mia Chen, HyoukJoong  
634 Lee, Jiquan Ngiam, Quoc V Le, Yonghui Wu, et al. Gpipe: Efficient training of giant neural  
635 networks using pipeline parallelism. *Advances in neural information processing systems*, 32,  
636 2019.
- 637 Sam Ade Jacobs, Masahiro Tanaka, Chengming Zhang, Minjia Zhang, Leon Song, Samyam Ra-  
638 jbandari, and Yuxiong He. DeepSpeed Ulysses: System optimizations for enabling training of  
639 extreme long sequence transformer models. *arXiv preprint arXiv:2309.14509*, 2023.
- 640 Peng Jin, Ryuichi Takanobu, Caiwan Zhang, Xiaochun Cao, and Li Yuan. Chat-univi: Unified visual  
641 representation empowers large language models with image and video understanding. *CoRR*,  
642 abs/2311.08046, 2023.

- 648 Jing Yu Koh, Robert Lo, Lawrence Jang, Vikram Duvvur, Ming Chong Lim, Po-Yu Huang, Graham  
649 Neubig, Shuyan Zhou, Ruslan Salakhutdinov, and Daniel Fried. Visualwebarena: Evaluating  
650 multimodal agents on realistic visual web tasks. *arXiv preprint arXiv:2401.13649*, 2024.  
651
- 652 Vijay Anand Korthikanti, Jared Casper, Sangkug Lym, Lawrence McAfee, Michael Andersch, Mo-  
653 hammad Shoeybi, and Bryan Catanzaro. Reducing activation recomputation in large transformer  
654 models. *Proceedings of Machine Learning and Systems*, 5:341–353, 2023.
- 655 Dmitry Lepikhin, HyoukJoong Lee, Yuanzhong Xu, Dehao Chen, Orhan Firat, Yanping Huang,  
656 Maxim Krikun, Noam Shazeer, and Zhifeng Chen. Gshard: Scaling giant models with conditional  
657 computation and automatic sharding. *arXiv preprint arXiv:2006.16668*, 2020.  
658
- 659 Bo Li, Yuanhan Zhang, Dong Guo, Renrui Zhang, Feng Li, Hao Zhang, Kaichen Zhang, Yanwei Li,  
660 Ziwei Liu, and Chunyuan Li. Llava-onevision: Easy visual task transfer. *CoRR*, abs/2408.03326,  
661 2024a.
- 662 Dacheng Li, Rulin Shao, Anze Xie, Eric Xing, Joseph Gonzalez, Ion Stoica, Xuezhe Ma, and Hao  
663 Zhang. Lightseq: : Sequence level parallelism for distributed training of long context transform-  
664 ers. In *Workshop on Advancing Neural Network Training: Computational Efficiency, Scalability,*  
665 *and Resource Optimization*, 2023a.  
666
- 667 Junnan Li, Dongxu Li, Silvio Savarese, and Steven Hoi. Blip-2: Bootstrapping language-  
668 image pre-training with frozen image encoders and large language models. *arXiv preprint*  
669 *arXiv:2301.12597*, 2023b.
- 670 Kunchang Li, Yinan He, Yi Wang, Yizhuo Li, Wenhai Wang, Ping Luo, Yali Wang, Limin Wang,  
671 and Yu Qiao. Videochat: Chat-centric video understanding. *CoRR*, abs/2305.06355, 2023c.  
672
- 673 Kunchang Li, Yali Wang, Yinan He, Yizhuo Li, Yi Wang, Yi Liu, Zun Wang, Jilan Xu, Guo Chen,  
674 Ping Lou, Limin Wang, and Yu Qiao. Mvbench: A comprehensive multi-modal video under-  
675 standing benchmark. In *CVPR*, pp. 22195–22206, 2024b.
- 676 Shenggui Li, Fuzhao Xue, Chaitanya Baranwal, Yongbin Li, and Yang You. Sequence parallelism:  
677 Long sequence training from system perspective. *arXiv preprint arXiv:2105.13120*, 2021.  
678
- 679 Yanwei Li, Yuechen Zhang, Chengyao Wang, Zhisheng Zhong, Yixin Chen, Ruihang Chu, Shaoteng  
680 Liu, and Jiaya Jia. Mini-gemini: Mining the potential of multi-modality vision language models,  
681 2024c.
- 682 Bin Lin, Yang Ye, Bin Zhu, Jiayi Cui, Munan Ning, Peng Jin, and Li Yuan. Video-llava: Learning  
683 united visual representation by alignment before projection. *CoRR*, abs/2311.10122, 2023a.  
684
- 685 Ji Lin, Hongxu Yin, Wei Ping, Yao Lu, Pavlo Molchanov, Andrew Tao, Huizi Mao, Jan Kautz,  
686 Mohammad Shoeybi, and Song Han. Vila: On pre-training for visual language models, 2023b.
- 687 Hao Liu, Matei Zaharia, and Pieter Abbeel. Ring attention with blockwise transformers for near-  
688 infinite context. *arXiv preprint arXiv:2310.01889*, 2023a.  
689
- 690 Hao Liu, Wilson Yan, Matei Zaharia, and Pieter Abbeel. World model on million-length video and  
691 language with blockwise ringattention. *arXiv preprint arXiv:2402.08268*, 2024a.
- 692 Haotian Liu, Chunyuan Li, Yuheng Li, and Yong Jae Lee. Improved baselines with visual instruction  
693 tuning. *arXiv preprint arXiv:2310.03744*, 2023b.  
694
- 695 Haotian Liu, Chunyuan Li, Qingyang Wu, and Yong Jae Lee. Visual instruction tuning. In *NeurIPS*,  
696 2023c.
- 697 Haotian Liu, Chunyuan Li, Yuheng Li, Bo Li, Yuanhan Zhang, Sheng Shen, and Yong Jae Lee.  
698 Llava-next: Improved reasoning, ocr, and world knowledge, January 2024b.  
699
- 700 Jiajun Liu, Yibing Wang, Hanghang Ma, Xiaoping Wu, Xiaoqi Ma, xiaoming Wei, Jianbin Jiao,  
701 Enhua Wu, and Jie Hu. Kangaroo: A powerful video-language model supporting long-context  
video input. *arXiv preprint arXiv:2408.15542*, 2024c.



- 702 Muhammad Maaz, Hanoona Rasheed, Salman Khan, and Fahad Shahbaz Khan. Video-chatgpt:  
703 Towards detailed video understanding via large vision and language models. In *Proceedings of*  
704 *the 62nd Annual Meeting of the Association for Computational Linguistics (ACL 2024)*, 2024.  
705
- 706 Karttikeya Mangalam, Raiymbek Akshulakov, and Jitendra Malik. Egoschema: A diagnostic bench-  
707 mark for very long-form video language understanding. In *NeurIPS*, 2023.
- 708 Deepak Narayanan, Aaron Harlap, Amar Phanishayee, Vivek Seshadri, Nikhil R Devanur, Gre-  
709 gory R Ganger, Phillip B Gibbons, and Matei Zaharia. Pipedream: Generalized pipeline par-  
710 allelism for dnn training. In *Proceedings of the 27th ACM symposium on operating systems*  
711 *principles*, pp. 1–15, 2019.  
712
- 713 Long Ouyang, Jeffrey Wu, Xu Jiang, Diogo Almeida, Carroll Wainwright, Pamela Mishkin, Chong  
714 Zhang, Sandhini Agarwal, Katarina Slama, Alex Ray, et al. Training language models to fol-  
715 low instructions with human feedback. *Advances in neural information processing systems*, 35:  
716 27730–27744, 2022.
- 717 Abhishek Padalkar, Acorn Pooley, Ajinkya Jain, Alex Bewley, Alex Herzog, Alex Irpan, Alexander  
718 Khazatsky, Anant Rai, Anikait Singh, Anthony Brohan, et al. Open x-embodiment: Robotic  
719 learning datasets and rt-x models. *arXiv preprint arXiv:2310.08864*, 2023.  
720
- 721 Viorica Patraucean, Lucas Smaira, Ankush Gupta, Adrià Recasens, Larisa Markeeva, Dylan Ba-  
722 narse, Skanda Koppula, Joseph Heyward, Mateusz Malinowski, Yi Yang, Carl Doersch, Tatiana  
723 Matejovicova, Yury Sulsky, Antoine Miech, Alexandre Fréchet, Hanna Klimczak, Raphael  
724 Koster, Junlin Zhang, Stephanie Winkler, Yusuf Aytar, Simon Osindero, Dima Damen, Andrew  
725 Zisserman, and João Carreira. Perception test: A diagnostic benchmark for multimodal video  
726 models. In *NeurIPS*, 2023.
- 727 Samyam Rajbhandari, Jeff Rasley, Olatunji Ruwase, and Yuxiong He. Zero: Memory optimizations  
728 toward training trillion parameter models. In *SC20: International Conference for High Perfor-*  
729 *mance Computing, Networking, Storage and Analysis*, pp. 1–16. IEEE, 2020.  
730
- 731 Share. Sharegemini: Scaling up video caption data for multimodal large language models, June  
732 2024.
- 733 Mohammad Shoeybi, Mostofa Patwary, Raul Puri, Patrick LeGresley, Jared Casper, and Bryan  
734 Catanzaro. Megatron-lm: Training multi-billion parameter language models using model par-  
735 allelism. *arXiv preprint arXiv:1909.08053*, 2019.  
736
- 737 Daria Soboleva, Faisal Al-Khateeb, Robert Myers, Jacob R Steeves, Joel Hestness, and Nolan Dey.  
738 SlimPajama: A 627B token cleaned and deduplicated version of RedPajama, 2023.
- 739 Jianlin Su, Yu Lu, Shengfeng Pan, Bo Wen, and Yunfeng Liu. Roformer: Enhanced transformer  
740 with rotary position embedding. *CoRR*, abs/2104.09864, 2021.  
741
- 742 Chameleon Team. Chameleon: Mixed-modal early-fusion foundation models. *arXiv preprint*  
743 *arXiv:2405.09818*, 2024.
- 744 Philippe Tillet, Hsiang-Tsung Kung, and David Cox. Triton: an intermediate language and compiler  
745 for tiled neural network computations. In *Proceedings of the 3rd ACM SIGPLAN International*  
746 *Workshop on Machine Learning and Programming Languages*, pp. 10–19, 2019.  
747
- 748 Shengbang Tong, Ellis Brown, Penghao Wu, Sanghyun Woo, Manoj Middepogu, Sai Charitha  
749 Akula, Jihan Yang, Shusheng Yang, Adithya Iyer, Xichen Pan, Austin Wang, Rob Fergus, Yann  
750 LeCun, and Saining Xie. Cambrian-1: A fully open, vision-centric exploration of multimodal  
751 llms, 2024.
- 752 Yuetian Weng, Mingfei Han, Haoyu He, Xiaojun Chang, and Bohan Zhuang. Longvlm: Efficient  
753 long video understanding via large language models. *CoRR*, abs/2404.03384, 2024.  
754
- 755 Haoning Wu, Dongxu Li, Bei Chen, and Junnan Li. Longvideobench: A benchmark for long-context  
interleaved video-language understanding. *CoRR*, abs/2407.15754, 2024.

- 756 Junbin Xiao, Xindi Shang, Angela Yao, and Tat-Seng Chua. Next-qa: Next phase of question-  
757 answering to explaining temporal actions. In *CVPR*, pp. 9777–9786, 2021.  
758
- 759 Lin Xu, Yilin Zhao, Daquan Zhou, Zhijie Lin, See-Kiong Ng, and Jiashi Feng. Pllava : Parameter-  
760 free llava extension from images to videos for video dense captioning. *CoRR*, abs/2404.16994,  
761 2024.
- 762 Hanrong Ye, De-An Huang, Yao Lu, Zhiding Yu, Wei Ping, Andrew Tao, Jan Kautz, Song Han, Dan  
763 Xu, Pavlo Molchanov, and Hongxu Yin. X-VILA: cross-modality alignment for large language  
764 model. *CoRR*, abs/2405.19335, 2024.  
765
- 766 Gyeong-In Yu, Joo Seong Jeong, Geon-Woo Kim, Soojeong Kim, and Byung-Gon Chun. Orca: A  
767 distributed serving system for {Transformer-Based} generative models. In *16th USENIX Sympo-  
768 sium on Operating Systems Design and Implementation (OSDI 22)*, pp. 521–538, 2022.
- 769 Zhou Yu, Dejing Xu, Jun Yu, Ting Yu, Zhou Zhao, Yueting Zhuang, and Dacheng Tao. Activitynet-  
770 qa: A dataset for understanding complex web videos via question answering. In *AAAI*, pp. 9127–  
771 9134, 2019.
- 772 Haoji Zhang, Yiqin Wang, Yansong Tang, Yong Liu, Jiashi Feng, Jifeng Dai, and Xiaojie Jin. Flash-  
773 vstream: Memory-based real-time understanding for long video streams. *CoRR*, abs/2406.08085,  
774 2024a.  
775
- 776 Peiyuan Zhang, Kaichen Zhang, Bo Li, Guangtao Zeng, Jingkang Yang, Yuanhan Zhang, Ziyue  
777 Wang, Haoran Tan, Chunyuan Li, and Ziwei Liu. Long context transfer from language to vision.  
778 *CoRR*.
- 779 Peiyuan Zhang, Kaichen Zhang, Bo Li, Guangtao Zeng, Jingkang Yang, Yuanhan Zhang, Ziyue  
780 Wang, Haoran Tan, Chunyuan Li, and Ziwei Liu. Long context transfer from language to vision.  
781 *arXiv preprint arXiv:2406.16852*, 2024b.  
782
- 783 Ruohong Zhang, Liangke Gui, Zhiqing Sun, Yihao Feng, Keyang Xu, Yuanhan Zhang, Di Fu, Chun-  
784 yuan Li, Alexander Hauptmann, Yonatan Bisk, and Yiming Yang. Direct preference optimization  
785 of video large multimodal models from language model reward, 2024c.
- 786 Yi-Fan Zhang, Qingsong Wen, Chaoyou Fu, Xue Wang, Zhang Zhang, Liang Wang, and Rong Jin.  
787 Beyond llava-hd: Diving into high-resolution large multimodal models. *CoRR*, abs/2406.08487,  
788 2024d.
- 789 Yanli Zhao, Andrew Gu, Rohan Varma, Liang Luo, Chien-Chin Huang, Min Xu, Less Wright,  
790 Hamid Shojanazeri, Myle Ott, Sam Shleifer, et al. Pytorch fsdp: experiences on scaling fully  
791 sharded data parallel. *arXiv preprint arXiv:2304.11277*, 2023.  
792
- 793 Zijia Zhao, Haoyu Lu, Yuqi Huo, Yifan Du, Tongtian Yue, Longteng Guo, Bingning Wang, Weipeng  
794 Chen, and Jing Liu. Needle in a video haystack: A scalable synthetic framework for benchmarking  
795 video mllms. *arXiv preprint*, 2024.
- 796 Lianmin Zheng, Wei-Lin Chiang, Ying Sheng, Siyuan Zhuang, Zhanghao Wu, Yonghao Zhuang,  
797 Zi Lin, Zhuohan Li, Dacheng Li, Eric. P Xing, Hao Zhang, Joseph E. Gonzalez, and Ion Stoica.  
798 Judging llm-as-a-judge with mt-bench and chatbot arena, 2023.  
799
- 800 Chunting Zhou, Pengfei Liu, Puxin Xu, Srinivasan Iyer, Jiao Sun, Yuning Mao, Xuezhe Ma, Avia  
801 Efrat, Ping Yu, Lili Yu, et al. Lima: Less is more for alignment. *Advances in Neural Information  
802 Processing Systems*, 36, 2024.
- 803 Luowei Zhou, Chenliang Xu, and Jason J. Corso. Towards automatic learning of procedures from  
804 web instructional videos. In *AAAI*, pp. 7590–7598, 2018.  
805
- 806 Zilin Zhu. Ring flash attention, 2023. Accessed: 2024-07-28.  
807  
808  
809

A APPENDIX

A.1 LONGVILA-CAPTION

We have developed a long video captioning benchmark, LongVILA-Caption, consisting of 100 long videos, with captions generated as detailed in Section 3.3, and verified through human examination. In line with the methodology of VideoChatGPT (Maaz et al., 2024), we evaluate the predictions of each model based on their correctness, detailed orientation, and contextual understanding. For instance, we assess correctness by employing GPT-4 to predict scores using a specific prompt. Additionally, we present two examples in Figures 13 and 14, featuring long videos in sports and technology. These examples demonstrate that LongVILA, with its capability to process more frames, offers a more comprehensive understanding of videos compared to its short-frame counterpart.

The Table 6 presents the performance metrics for the LongVILA models being trained and evaluated on varying numbers of frames: 8, 128, and 256. As the number of frames increases, the model’s performance improves significantly. Specifically, the average scores rise from 2.00 to 3.26, highlighting the model’s enhanced capability in generating accurate and rich captions with more frames.

Table 5: Iteration time (seconds) on the dataset (Chen et al., 2024a) with and without our two-stage sharding strategy.

	2 GPUs	4 GPUs	8 GPUs
one-stage	0.78	0.89	1.20
two-stage	0.77	0.86	1.12

Table 6: Evaluation of LongVILA-Caption performance across different frame counts.

Frames	Correctness	Detailed	Contextual	Average
8	1.87	1.85	2.27	2.00
128	2.36	2.44	2.79	2.53
256	3.23	3.11	3.43	3.26

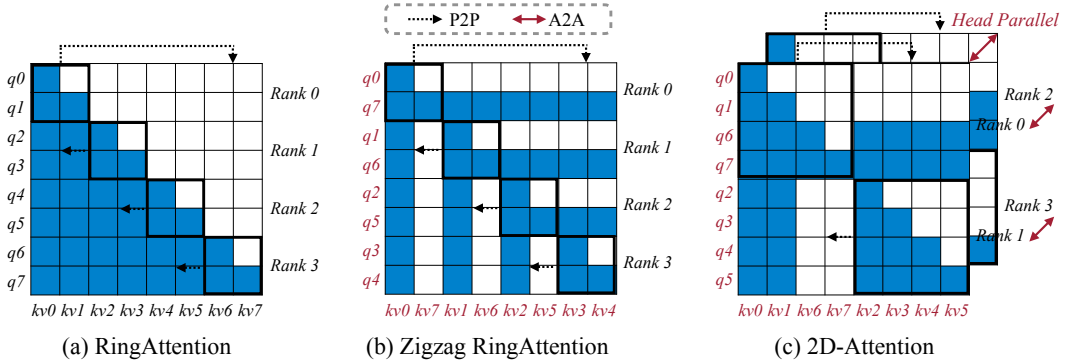


Figure 11: Comparison of RingAttention Liu et al. (2023a), ZIGZAG-RINGATTN Zhu (2023), and 2D-Attention (Fang & Zhao, 2024). The blue block indicates communication between QKV, while the black frame represents local attention computation within each SP group rank. The sequence length is 8 and the global SP degree is 4. Due to the triangular structure of causal attention computations, RingAttention experiences a computation imbalance, where rank 0 becomes idle after the first round while rank 3 continues computing through all stages. ZIGZAG-RINGATTN addresses this by reordering input sequence tokens along the sequence dimension to achieve load balance. The 2D-Attention mechanism uses a ring parallel degree of 2 and a head parallel degree of 2, resulting in an effective global sequence parallel degree of 4. This approach also incorporates a workload balancing strategy within the ring-based process group and uses the All-to-All operation to distribute QKV tensors across devices based on the head dimension, ensuring efficient and balanced computation.

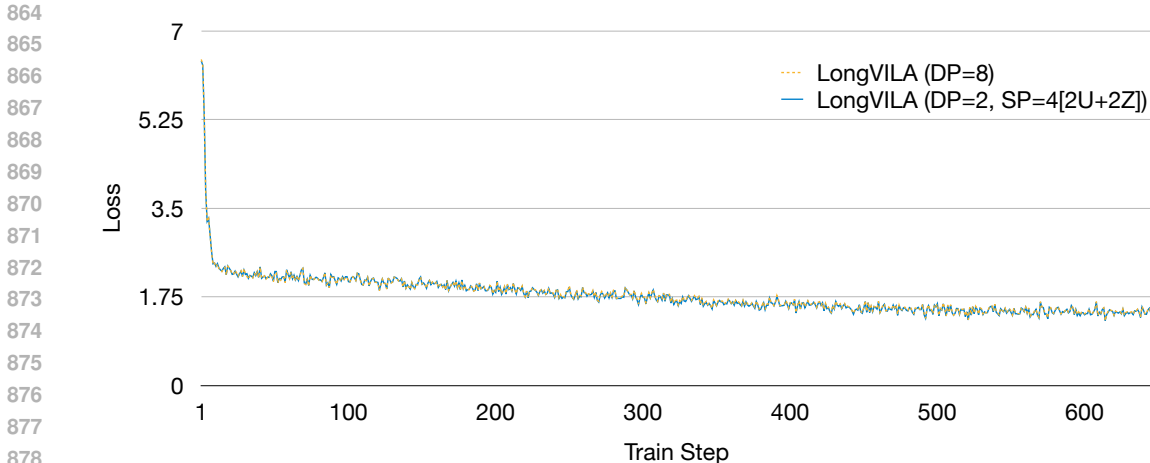


Figure 12: Convergence evaluation. We compare the training loss curves for LongVILA with and without sequence parallelism. This figure illustrates the convergence of the LongVILA model on 8 H100 GPUs, with a sequence parallelism degree of 4, compared to pure data parallelism training. 2U+2Z indicates that 2D-Attention mechanism is enabled, where both the Ulysses and Zigzag-Ringtn degrees are 2. The training dataset is shot2story. The two curves align closely, indicating that our MM-SP system does not negatively impact training quality.

Table 7: Our training system, used in conjunction with FSDP (Zhao et al., 2023) or Zero-3 (Rajbhandari et al., 2020), on 32 H100 GPUs. We found that FSDP offers more efficient memory management, which led us to select it as our default configuration. (Time per iteration, seconds).

Sequence Length	Zero-3			FSDP		
	ZIGZAG-RINGATTN	Ulysses	2D Attention	ZIGZAG-RINGATTN	Ulysses	2D Attention
320 K	OOM	OOM	OOM	23.57	10.70	11.12
288 K	OOM	OOM	OOM	20.24	8.68	8.65
256 K	OOM	OOM	OOM	17.54	6.98	7.04
224 K	19.04	7.06	5.73	15.22	5.47	5.53
192 K	13.01	4.24	4.38	12.97	4.15	4.24
160 K	10.73	3.09	3.23	10.83	3.02	3.11
128 K	8.63	2.16	2.30	8.38	2.07	2.17
96 K	6.49	1.43	1.53	6.35	1.33	1.41
64 K	4.40	1.01	1.08	4.25	0.76	0.80
32 K	2.06	1.58	1.04	2.26	0.39	0.40

Table 8: Training system throughput comparison on 64 H100 GPUs, measured in time per iteration (seconds). Ulysses is not included in this comparison as it supports only up to 32 GPUs.

Sequence length	Megatron-LM		Ours		
	CP	CP=8+TP=8	ZIGZAG-RINGATTN	Ulysses	2D Attention
640 K	OOM	OOM	88.4	-	OOM
578 K	OOM	OOM	77.2	-	16.9
512 K	OOM	OOM	66.1	-	13.31
448 K	OOM	OOM	57.5	-	10.39
384 K	OOM	OOM	48.6	-	7.80
320 K	OOM	OOM	40.5	-	5.63
256 K	OOM	5.31	32.2	-	3.93
192 K	8.81	3.10	24.1	-	2.49
128 K	7.10	1.57	16.0	-	1.36
64 K	3.09	0.61	8.04	-	0.57
32 K	1.86	0.44	4.24	-	0.33

918  
919  
920  
921  
922  
923  
924  
925  
926  
927  
928  
929  
930  
931  
932  
933  
934  
935  
936  
937  
938  
939  
940  
941  
942  
943  
944  
945  
946  
947  
948  
949  
950  
951  
952  
953  
954  
955  
956  
957  
958  
959  
960  
961  
962  
963  
964  
965  
966  
967  
968  
969  
970  
971

Table 9: Comparison with state-of-the-art methods (Li et al., 2023b; Dai et al., 2023; Bai et al., 2023; Liu et al., 2023b; Lin et al., 2023b; Liu et al., 2024b; Tong et al., 2024; Li et al., 2024c) on 10 image based VLM benchmarks. S3 refers to the stage 3 model in LongVILA training pipeline.

Method	LLM	Res.	VQA <sup>v2</sup>	GQA	VizWiz	SQA <sup>l</sup>	VQA <sup>T</sup>	MMB	MMB <sup>CN</sup>	SEED	LLaVA <sup>W</sup>	MM-Vet
BLIP-2	Vicuna-13B	224	41.0	41	19.6	61	42.5	-	-	46.4	38.1	22.4
InstructBLIP	Vicuna-7B	224	-	49.2	34.5	60.5	50.1	36	23.7	53.4	60.9	26.2
	Vicuna-13B	224	-	49.5	33.4	63.1	50.7	-	-	-	58.2	25.6
Qwen-VL	Qwen-7B	448	78.8	59.3	35.2	67.1	63.8	38.2	7.4	56.3	-	-
	Qwen-VL-Chat	448	78.2	57.5	38.9	68.2	61.5	60.6	56.7	58.2	-	-
LLaVA-1.5	Vicuna-1.5-7B	336	78.5	62.0	50.0	66.8	58.2	64.3	58.3	58.6	63.4	30.5
	Vicuna-1.5-13B	336	80.0	63.3	53.6	71.6	61.3	67.7	63.6	61.6	70.7	35.4
VILA	Llama 2-7B	336	79.9	62.3	57.8	68.2	64.4	68.9	61.7	61.1	69.7	34.9
	Llama 2-13B	336	80.8	63.3	60.6	73.7	66.6	70.3	64.3	62.8	73.0	38.8
LLaVA-NeXT-8B	Llama 3-8B	672	-	65.2	-	72.8	64.6	72.1	-	-	80.1	-
Cambrian-1-8B	Llama 3-8B	1024	-	64.6	-	80.4	71.7	75.9	-	-	-	-
Mini-Gemini-HD-8B	Llama 3-8B	1536	-	64.5	-	75.1	70.2	72.7	-	-	-	-
LongVILA-7B (S3)	Qwen2-7B	dynamic	<b>85.4</b>	<b>65.4</b>	<b>65.0</b>	<b>98.5</b>	<b>77.8</b>	<b>83.4</b>	<b>80.0</b>	<b>70.6</b>	<b>77.6</b>	<b>51.7</b>

Table 10: Detailed model complexity analysis of LongVILA among various model size, number of frames, parameters, latency (ms), and TFLOPs. We profile LongVILA models into 4 types of components. Image Encoder includes vision tower and mm projector. LLM Linears include k/q/v/o projectors and linears in decoder layers. LLM Attention is the attention computation. LLM Others include other components, like embeddings, output heads, and normalization layers. We use fp16 data type, Flash-Attention2 (Dao, 2024) on one A100 GPU for latency measurement. As the number of frames increases, the FLOPs and latency of LLM Attention grow quadratically, whereas other components increase linearly. LLM Attention represents the predominant computational cost in long video understanding, highlighting the MM-SP system.

Frames	Context	Metric	LongVILA-1.5B				LongVILA-7B			
			Image Encoder	LLM Linears	LLM Attention	LLM Others	Image Encoder	LLM Linears	LLM Attention	LLM Others
		Params	0.44B	1.31B	-	0.23B	0.46B	6.53B	-	1.09B
32	6415	Latency	196.0	109.3	27.0	28.9	201.0	426.2	51.1	42.1
		TFLOPs	5.13	4.20	1.77	0.75	5.22	20.93	4.13	1.74
64	12719	Latency	375.2	208.1	80.7	50.9	375.8	831.1	173.8	80.8
		TFLOPs	10.26	8.33	6.96	1.48	10.45	41.50	16.24	3.46
128	25327	Latency	740.4	403.2	288.1	97.1	755.1	1642.4	644.9	158.3
		TFLOPs	20.52	16.60	27.59	2.95	20.89	82.64	64.38	6.89
256	50543	Latency	1456.0	811.2	1087.7	192.5	1476.3	3308.2	2529.6	325.1
		TFLOPs	41.05	33.12	109.89	5.88	41.78	164.92	256.40	13.74
512	100975	Latency	2921.0	1660.9	4359.2	389.4	2980.2	6675.1	10149.3	653.4
		TFLOPs	82.09	66.17	438.59	11.75	83.57	329.48	1023.37	27.45



972  
973  
974  
975  
976  
977  
978  
979  
980  
981  
982  
983  
984  
985  
986  
987  
988  
989  
990  
991  
992  
993  
994  
995  
996  
997  
998  
999  
1000  
1001  
1002  
1003  
1004  
1005  
1006  
1007  
1008  
1009  
1010  
1011  
1012  
1013  
1014  
1015  
1016  
1017  
1018  
1019  
1020  
1021  
1022  
1023  
1024  
1025



Elaborate on the visual and narrative elements of the video in detail. <Video> : 



8 frames

**The video opens with a scene of two soccer players in blue jerseys standing on a green field, with one of them holding a soccer ball.** The next scene shows a goalkeeper in a green jersey diving to save a goal. Following this, there is a clip of a player in a red jersey falling to the ground, possibly after a tackle. The subsequent scene captures a player in a red jersey running with the ball towards the goal. The video then transitions to a wide shot of a soccer field with players in red and white jerseys, and a crowd in the stands. The final scene displays a logo with the text "BUNDESLIGA" and a call to action to "CLICK HERE TO SUBSCRIBE!"

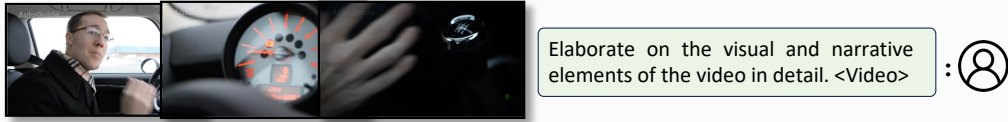


256 frames

**The video begins with a soccer game being played on a field, where players in blue and red jerseys are seen, with the ball being passed around and occasionally kicked.** The camera focuses on different players, including one in a blue jersey who scores a goal. The scene shifts to a celebration with a player in a blue jersey holding his hands up, followed by a shot of a number 10. The game continues with players in green and white jerseys, and the camera captures various moments, including goals being scored and players running on the field. **At one point, the players are seen hugging each other.** The video transitions to a series of shots that include numbers against a white background, followed by more scenes of the soccer game. The players are now wearing red and white jerseys, and the crowd is cheering enthusiastically. The video also features close-ups of individual players and moments of celebration, such as a player in a red jersey being congratulated by teammates. Towards the end, the camera shows a man in a black jacket walking on the field, and then cuts to three men standing together. Finally, the video concludes with a man in a black T-shirt talking to the camera, with a red and white logo appearing on the screen.

Figure 13: Examples of sports long video caption with LongVILA. For the gameplay opening, the 8-frame baseline describes only static image, two players in only blue jerseys. In contrast, 256-frame LongVILA describes players in blue and red jerseys passing and kicking the ball. In addition, the 256-frame version also include the detail of players hugging emphasizes the celebratory aspects, which is missing in the 8-frame baseline.

1026  
1027  
1028  
1029  
1030  
1031  
1032  
1033  
1034  
1035  
1036  
1037  
1038  
1039  
1040  
1041  
1042  
1043  
1044  
1045  
1046  
1047  
1048  
1049  
1050  
1051  
1052  
1053  
1054  
1055  
1056  
1057  
1058  
1059  
1060  
1061  
1062  
1063  
1064  
1065  
1066  
1067  
1068  
1069  
1070  
1071  
1072  
1073  
1074  
1075  
1076  
1077  
1078  
1079



Elaborate on the visual and narrative elements of the video in detail. <Video>

8 frames

The video begins with a dark screen, followed by a series of images that highlight different features of a Mini Cooper. **The first image shows two Mini Coopers side by side**, with arrows pointing to specific features such as "Side Mirror Lens," "New Bumper Fascia," "Larger Fog Lights," and "Functional Brake Ducts." The cars are blue, and the text is in white with red arrows. The next image is a blurred motion shot of a Mini Cooper driving on a road with snow on the sides. The following image is a close-up of a car's air vent with a blurred background. Another image shows a man in a black coat and glasses, presumably a car expert, speaking inside a Mini Cooper, with the interior visible in the background. The subsequent image is a blurred shot of a white Mini Cooper parked in a garage. The final image is a dark screen with the text "FOR FULL REVIEW, VISIT: AutoGuide.com" in red and white.

256 frames

The video begins with a focus on a silver car's ignition button and **transitions to various shots of a white car driving on a snowy road, with close-ups of its front, rear, and side**. A man in a black coat is then introduced, standing next to a silver car in a garage, talking to the camera. The scene shifts to a showroom setting, showcasing two blue cars, followed by a man in a black coat discussing features in front of a laptop. The narrative continues with the man driving, detailing the car's interior and controls, including the dashboard, gear shift, and steering wheel. The video emphasizes the driving experience, with repeated shots of the man talking and gesturing while driving on a snowy road, with the camera occasionally focusing on the **car's dashboard, gauges, and controls. The sequence includes close-ups of the car's ignition button, gear shift, and a detailed view of the dashboard**. Towards the end, the video features the man in a black coat discussing the car's features in front of a white car parked in a garage, highlighting the headlights, wheels, and the car's interior. The video concludes with the man standing next to the white car in a dimly lit garage, continuing his dialogue with the camera.

Figure 14: Examples of technology long video caption with LongVILA. At the beginning of captions, the 8-frame baseline only describes static image and two cars. In contrast, the 256-frame LongVILA describes the car on snowy road, covering front, rear, and side views. For details, the 256-frame LongVILA describes close-ups of ignition button, gear shift, and dashboard elements, which are missing in the 8-frame baseline.